X-ray Diffraction from Magnetic Materials

Dr. Sonia Francoual
Resonant Scattering and Diffraction beamline P09, PETRA III
Deutsches Elektronen-Synchrotron, Hamburg, Germany
Hamburg, 05.10.2017

HELMHOLTZ | ASSOCIATION

DESY

Heading Agenda

Subheading, optional

1. **Single-crystal X-ray Diffraction**
2. **Single-crystal X-ray Diffraction from Magnetic Materials**
3. **Experimental Aspects**
4. **Scientific highlights**
5. **Conclusions**

Single-crystal X-ray diffraction

X-rays

W. Roentgen , Nobel Prize 1901

X-rays are photons, no mass, no charge;

Electromagnetic waves: $\widehat{E(\vec{r},t)} = \hat{\varepsilon} E_0(\vec{r},t) e^{i(\vec{k}\vec{r}-\omega t)}$

- Wavenumber $k = \frac{2\pi}{\lambda}$, frequency $\frac{\omega}{2\pi}$, polarization $\hat{\varepsilon}$
- Energy $E[keV] = \frac{12.39842}{\lambda}[\dot{A}]$

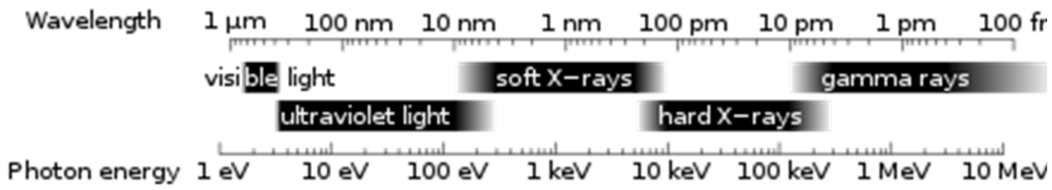

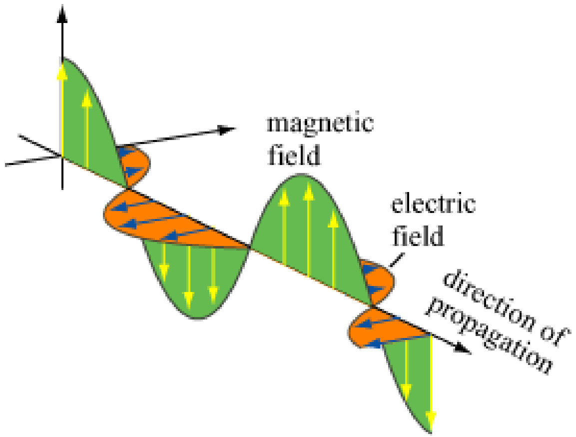

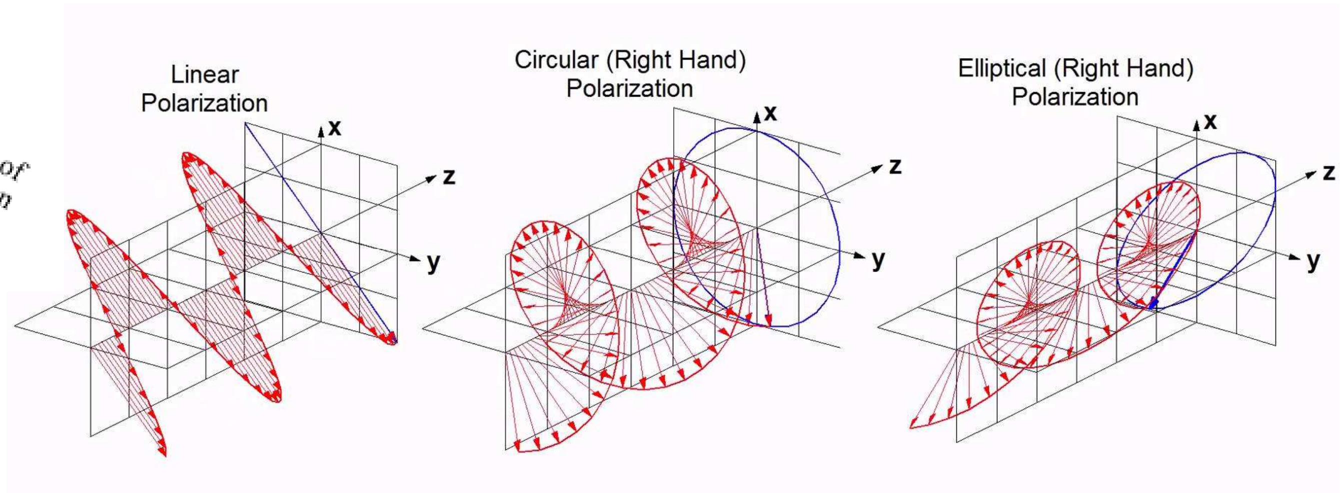

Interaction of X-rays with Matter

X-ray attenuation dominant processes / Total photon scattering cross-section

1) Absorption (w/o ionisation)
2) Photoelectric effect (ionisation of a valence or core electrons, secondary emission)
3) Coherent scattering (atoms nor ionized neither excited)
4) Compton scattering

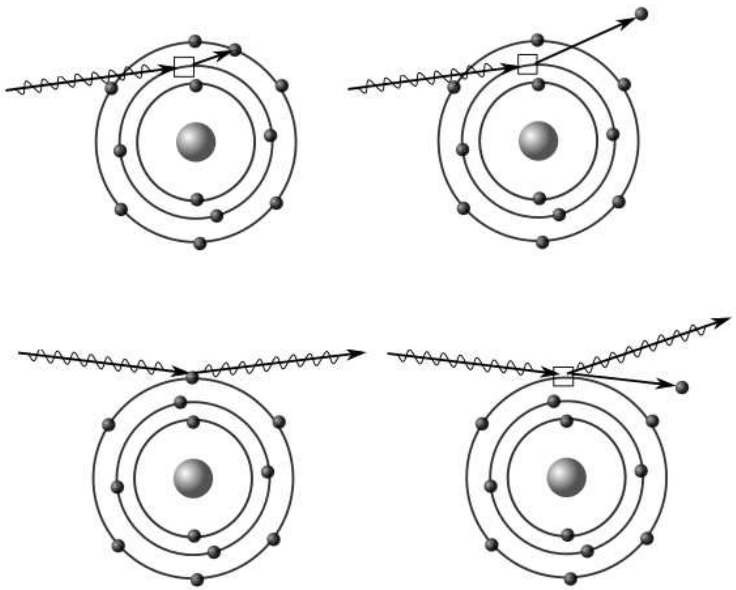

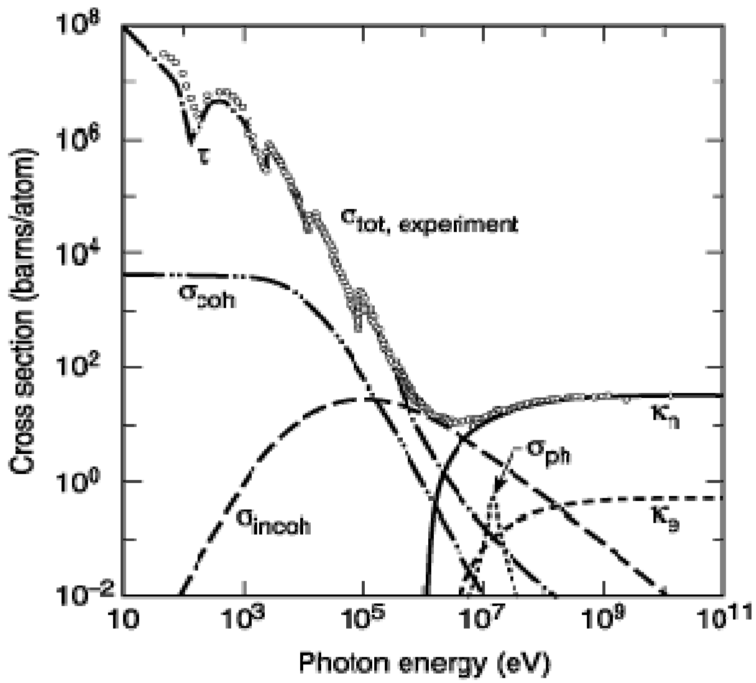

Thomson elastic scattering

J. J. Thomson, Nobel Prize 1906

X-rays are EM waves coupling to the charge of the electrons;

- Electromagnetic field interacts with outer shell electrons accelerating them, acceleration produces re-radiation at a same energy in all directions
- A plane-wave impinging on a quasi-free charge produces a scattered spherical wave with an amplitude that depends on the scattering angle
- The electric field due to an accelerated particle depends on the angle between the acceleration and the scattered radiation

Scattering by a free electron

$$\langle E^2\rangle / \langle E_0^2\rangle = \frac{e^4}{m^2 c^4 R^2}\left((1+\cos^2\phi)/2\right)$$

$\Rightarrow$ 1 mg of matter $\Rightarrow$ $I/I_0 \sim 10^{-5}$

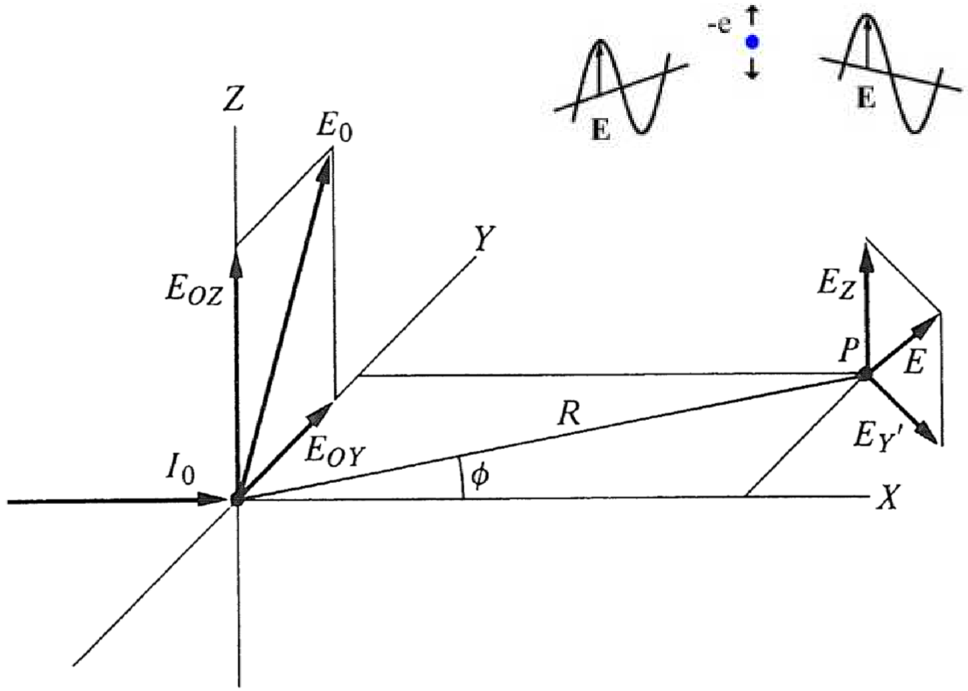

X-ray atomic form factor

Amplitude of a wave scattered by an isolated atom ~ sum of amplitudes per electrons

$$f \;=\int \rho(r) e^{iQr} d^3r = f_0 + f' + if''$$

$f_0 \rightarrow$ Z at small values of (sin θ)/λ

$f' + if''$: dispersion corrections close to at absorption edges, very weak dependence on the scattering angle, f'' represents a phase shift of the scattered photons

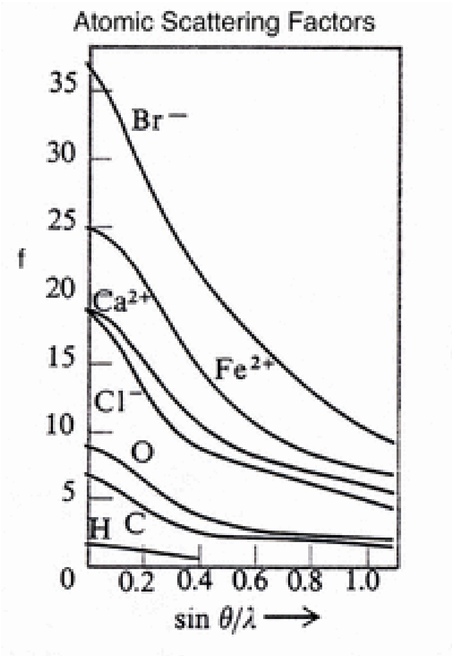

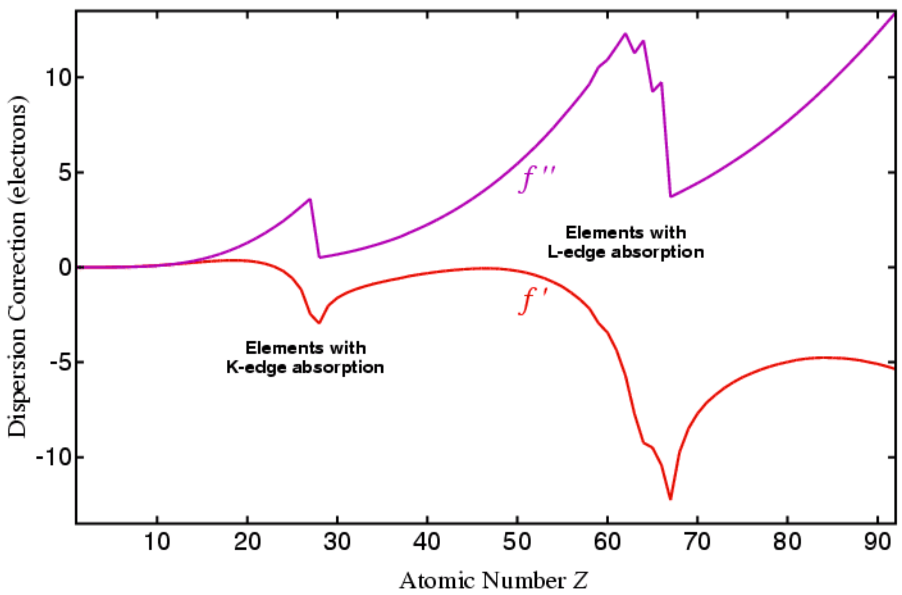

X-ray diffraction

Diffraction from a set of atoms, Bragg Law, Reciprocal space

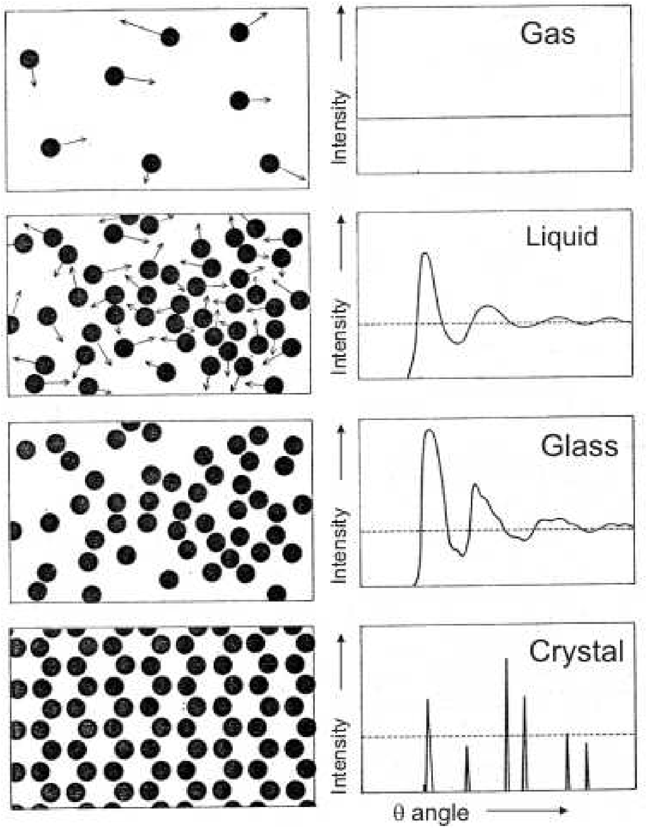

Crystals made up of parallel planes of atoms; incident waves specularly reflected by those planes; constructive interferences occurs when path difference is an integral number of wavelengths:

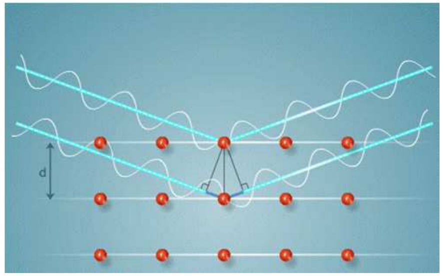

Bragg Law: $n\lambda = 2d_{hkl}sin\theta$

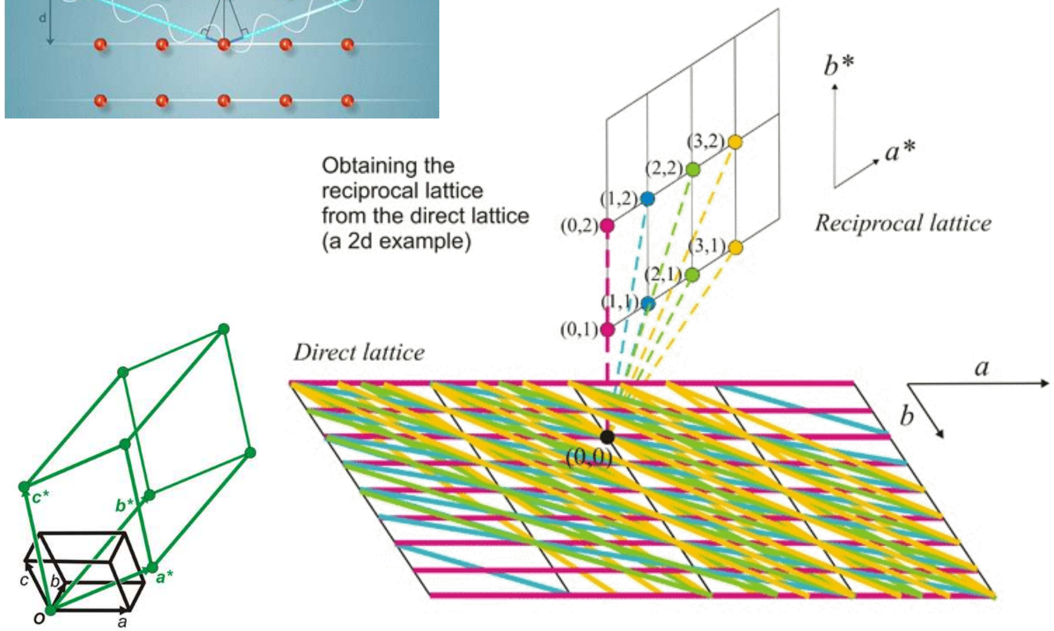

X-ray diffraction

Bravais lattice & Selection rules

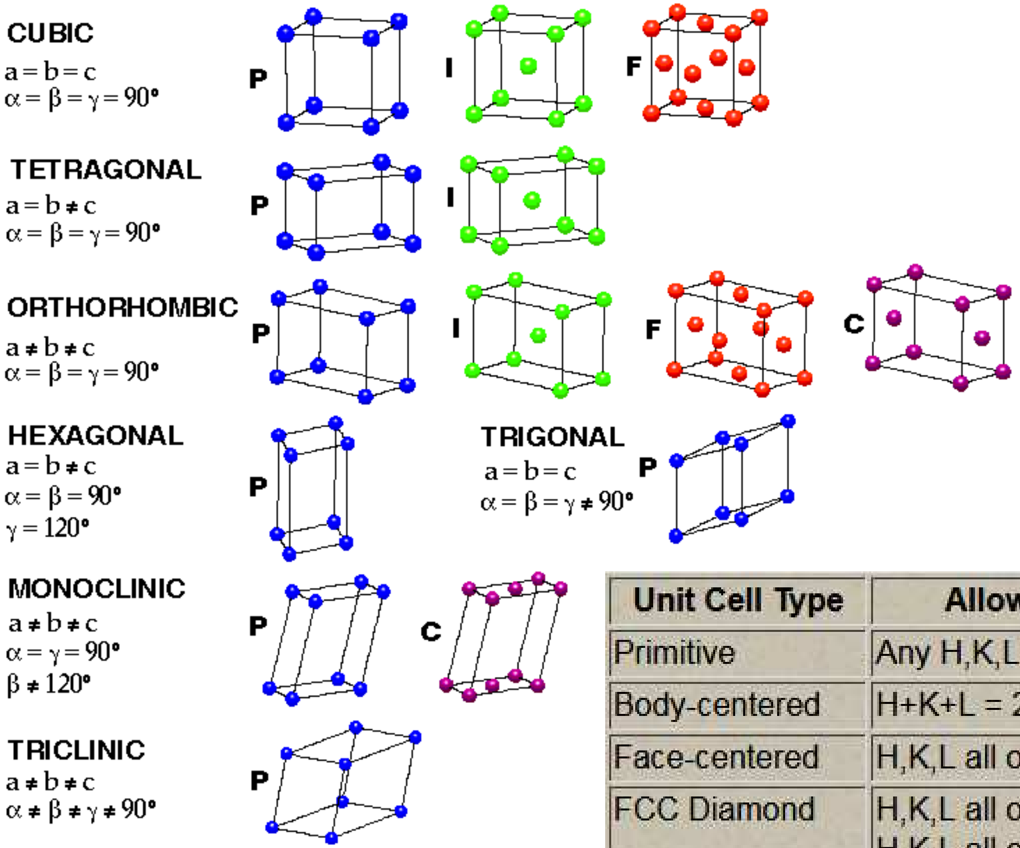

4 Types of Unit Cell
P = Primitive
I = Body-Centred
F = Face-Centred
C = Side-Centred
+
7 Crystal Classes
→ 14 Bravais Lattices

Unit Cell Type	Allowed Reflections	Forbidden Reflections
Primitive	Any H,K,L	None
Body-centered	H+K+L = 2n (even)	H+K+L = 2n+1 (odd)
Face-centered	H,K,L all odd or all even	H,K,L mixed odd, even
FCC Diamond	H,K,L all odd H,K,L all even and H+K+L = 4n	H,K,L mixed odd, even H,K,L all even and H+K+L ≠ 4n
Hexagonal (HCP)	L even H+2K ≠ 3n	L odd and H+2K = 3n

Single-crystal X-ray diffraction from magnetic materials

Ordering: crystalline, magnetic, orbital,….

Quasicrystals : 6D periodicity,…

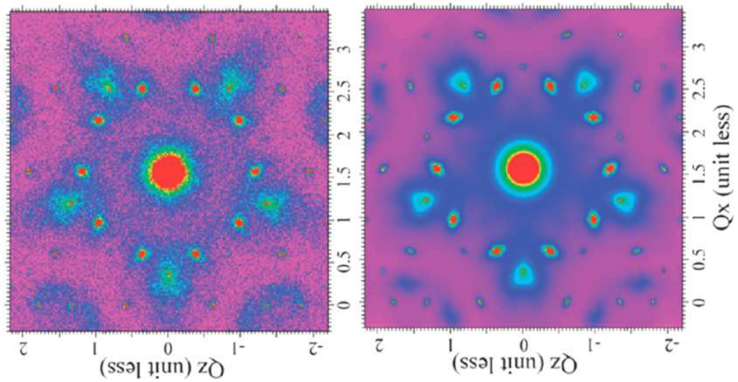

Magnetic ordering

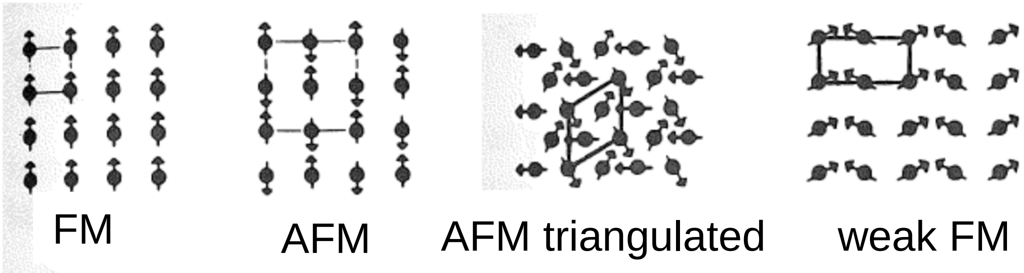

Orbital ordering

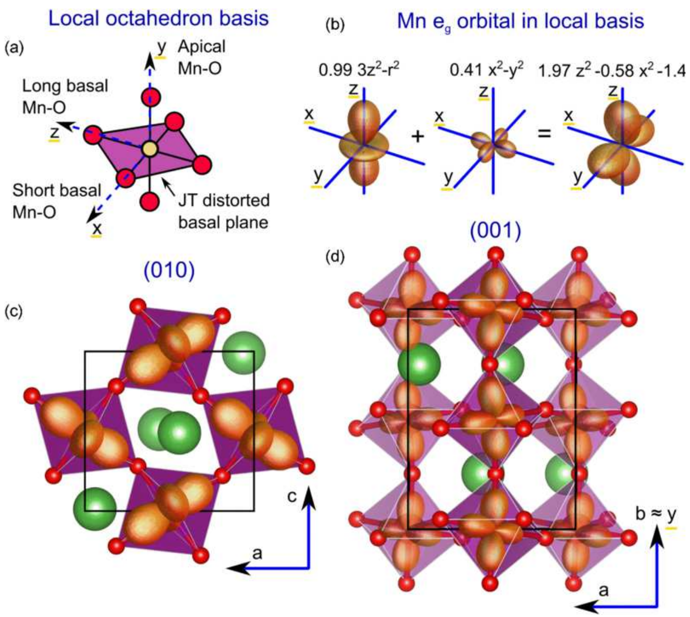

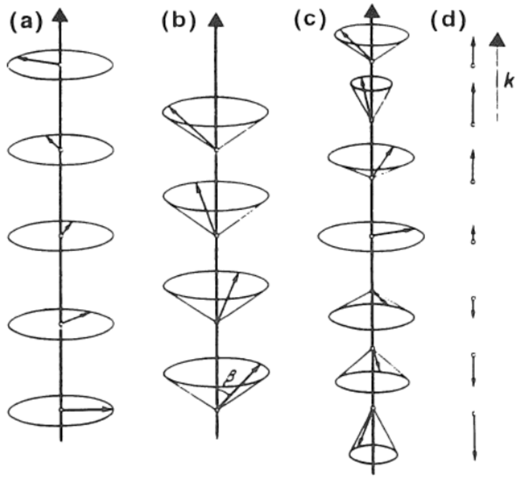

Incommensurate order: spiral, conical spiral, …

Diffraction from magnetic materials

Non-resonant magnetic scattering / pre-synchrotron work

In the nonrelativistic limit, X-rays couple exclusively to the charge of the electrons; however acceleration of an electron by a photon depends upon the spin as well;

- 1970: Platzman & Tsoar predict X-ray diffraction from antiferromagnets
- 1972 & 1974 till 1981,1984: Brunel & de Bergevin demonstrate experimentally the non resonant magnetic scattering from ferromagnets, ferrimagnets and antiferromagnets in the laboratory

F. de Bergevin & M. Brunel, Phys. Lett. A 39, 141 (1972)

Typically : $\frac{\sigma_{mag,NRXMS}}{\sigma_{charge}} \sim 10^{-6}$

General Formulae:

- de Bergevin & Brunel (1981)
- Blume and Gibbs (1988)

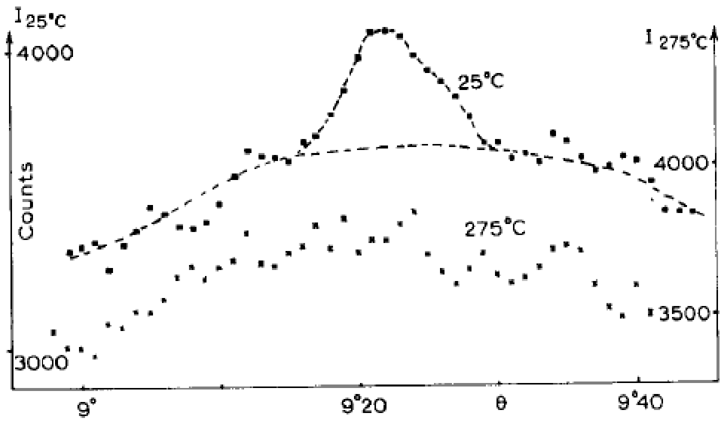

Fig. 1. Intensity $I_t(\theta)$ near the $(\frac{1}{2}\,\frac{1}{2}\,\frac{1}{2})$ position at $t = 25°$ C and 275° C in counts/225 min. The hump which cover the interval could be due to some impurity.

Diffraction from magnetic materials

Non-resonant X-ray magnetic scattering

$$\langle \mathbf{F}_m \rangle = -r_0 \frac{i\hbar\omega}{mc^2} \langle \mathbf{M}_m \rangle$$

$$\langle \mathbf{M}_m \rangle = \frac{1}{2} \mathbf{L}(\mathbf{Q}) \cdot \mathbf{A} + \mathbf{S}(\mathbf{Q}) \cdot \mathbf{B}$$

$$\mathbf{A} = 2(1 - \hat{k} \cdot \hat{k}')(\hat{\varepsilon}' \times \hat{\varepsilon}) - (\hat{k} \times \hat{\varepsilon})(\hat{k} \cdot \hat{\varepsilon}') + (\hat{k}' \times \hat{\varepsilon}')(\hat{k}' \cdot \hat{\varepsilon})$$

$$\boldsymbol{B} = (\hat{\varepsilon}' \times \hat{\varepsilon}) + (\hat{k}' \times \hat{\varepsilon}')(\hat{k}' \cdot \hat{\varepsilon}) - (\hat{k} \times \hat{\varepsilon})(\hat{k} \cdot \hat{\varepsilon}') - (\hat{k}' \times \hat{\varepsilon}') \cdot (\hat{k} \times \hat{\varepsilon})$$

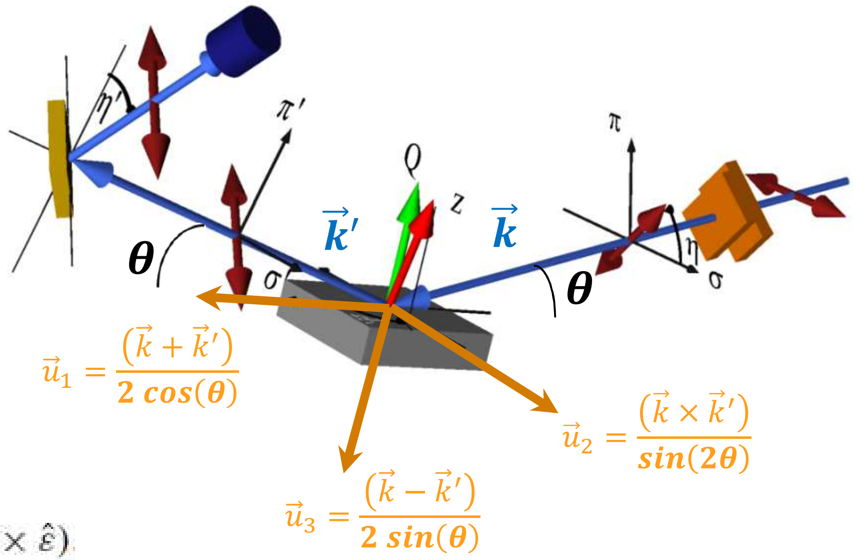

$$\langle \mathbf{M}_m \rangle = \begin{bmatrix} \langle M_m \rangle_{\sigma\sigma} & \langle M_m \rangle_{\sigma\pi} \\ \langle M_m \rangle_{\pi\sigma} & \langle M_m \rangle_{\pi\pi} \end{bmatrix} = \begin{bmatrix} (\sin 2\theta) S_2 & -2(\sin^2\theta)[(\cos\theta)(L_1+S_1) - (\sin\theta)S_3] \\ 2(\sin^2\theta)[(\cos\theta)(L_1+S_1) + (\sin\theta)S_3] & (\sin 2\theta)[2(\sin^2\theta)L_2 + S_2] \end{bmatrix}$$

- Weak but allows to obtain the L/S ratio
- High energy limit $\sin\theta \rightarrow 0 \;\Rightarrow\; S_2$ only

Diffraction from magnetic materials

Resonant X-ray magnetic scattering / work at synchrotron

- 1988 : Gibbs *et al.* observe a large resonant enhancement in the magnetic satellite intensities related to the magnetic spiral structure in Holmium when the energy of the incident X ray is tuned through the Ho L_{III} absorption edge
- 1988 : Hannon & Trammel explain the resonance enhancement as arising from electric multipole transitions

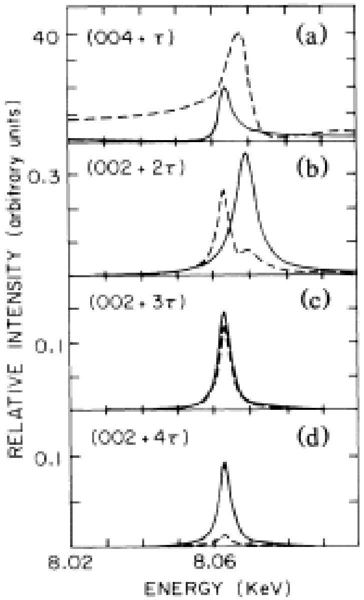

FIG. 1. Relative scattered intensities (theoretical) vs x-ray energy for the L_{III} edge in Ho: (a) $(004+\tau)$, (b) $(002+2\tau)$, (c) $(002+3\tau)$, and (d) $(002+4\tau)$. The solid lines give the $\sigma \leftrightarrow \sigma$ scattering, and the dashed lines give $\sigma \leftrightarrow \pi$.

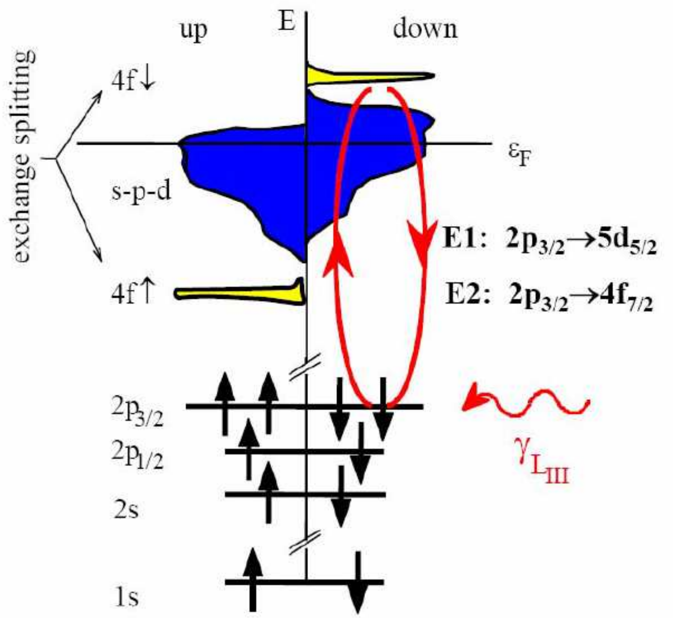

Diffraction from magnetic materials

Resonant X-ray magnetic scattering

Electric dipole and quadrupoles dominant processes; magnetic multipoles contributions smaller by a factor ~ 60;

$$f^{e}_{EL}(\omega) = \frac{4\pi}{k} f_{\mathrm{D}} \sum_{M=-L}^{L} [\hat{\varepsilon}'^{*} \cdot Y^{(e)}_{LM}(\hat{k}') Y^{(e)*}_{LM}(\hat{k}) \cdot \hat{\varepsilon}] F^{(e)}_{LM}(\omega)$$

E1 = Electric dipole transitions (L=1), E2 = Electric quadrupole transitions (L=2)

$$f^{\mathrm{XRES}}_{nE1} = F^{(0)} \begin{pmatrix} 1 & 0 \\ 0 & \cos 2\theta \end{pmatrix} - iF^{(1)} \begin{pmatrix} 0 & z_1 \cos\theta + z_3 \sin\theta \\ z_3 \sin\theta - z_1 \cos\theta & -z_2 \sin 2\theta \end{pmatrix} + F^{(2)} \begin{pmatrix} z_2^2 & -z_2(z_1 \sin\theta - z_3 \cos\theta) \\ +z_2(z_1 \sin\theta + z_3 \cos\theta) & -\cos^2\theta(z_1^2 \tan^2\theta + z_3^2) \end{pmatrix}, \quad (1$$

Series	Abs. edge	Energy (keV)	λ (Å)	Shells	Type	Resonant amplitude
3d	$L_{2,3}$	*0.4–1.0*	*12–30*	*2p→3d*	*E1*	*≈100*
	K	4.5–9.5	1.3–2.7	1s→4p	E1	≈0.02
				1s→3d	E2	≈0.01
5d	$L_{2,3}$	5.4–14	0.9–2.2	*2p→5d*	E1	≈1-10
4f	$L_{2,3}$	5.7–10.3	1.2–2.2	2p→5d	E1	≈0.10
				2p→4f	E2	≈0.05
	$M_{4,5}$	*0.9–1.6*	*7.7–13.8*	*2d→4f*	*E1*	*≈100-300*
5f	$L_{2,3}$	17–21	0.6–0.7	2p→6d	E1	≈0.05
				2p→4f	E2	≈0.01
	$M_{4,5}$	3.5–4.5	2.7–6	3d→5f	E1	≈10.0

⇒ Strong

⇒ electron and shell selective

⇒ Allows to probe ordering of several type of magnetic species in an alloy

Diffraction from magnetic materials

Resonant X-ray magnetic scattering

Di Matteo *et al.*, Phys. Rev. B 72 (2005) 144406

Multipolar order

Tensor	rank p	$\tilde{T}$	$\tilde{P}$	Type	Multipole
$F^{(0)}(E1-E1)$	0	+	+	charge	monopole
$F^{(0)}(E2-E2)$	0	+	+	charge	monopole
$F^{(1)}(E1-E1)$	1	-	+	magnetic	dipole
$F^{(1)}(E2-E2)$	1	-	+	magnetic	dipole
$F^{(1+)}(E1-E2)$	1	+	-	electric	dipole
$F^{(1-)}(E1-E2)$	1	-	-	polar toroidal	dipole
$F^{(2)}(E1-E1)$	2	+	+	electric	quadrupole
$F^{(2)}(E2-E2)$	2	+	+	electric	quadrupole
$F^{(2+)}(E1-E2)$	2	+	-	axial toroidal	quadrupole
$F^{(2-)}(E1-E2)$	2	-	-	magnetic	quadrupole
$F^{(3)}(E2-E2)$	3	-	+	magnetic	octupole
$F^{(3+)}(E1-E2)$	3	+	-	electric	octupole
$F^{(3-)}(E1-E2)$	3	-	-	polar toroidal	octupole
$F^{(4)}(E2-E2)$	4	+	+	electric	hexadecapole

$$f_j^{RXS} = \sum_{p,m}(-1)^{p+m} X_{-m}^{(p)} F_m^{(p)}(j;\omega)$$

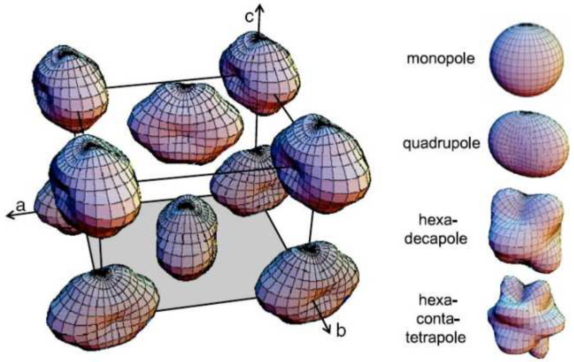

RXS has proved a powerful tool for probing multipolar ordering up to rank L=2 in CeB_6 [1,2] and in UO_2 [3], UPd_3 [4], DyB_2C_2 [5]. Field-induced octupolar ordering (L=3) is evidenced in CeB_6 at the Ce L_{III} edge upon applying magnetic fields [6].

[1] H. Nakao et al., J. Phys. Soc. Jpn. 70 (2001) 1857
[2] F. Yakhou et al., Phys. Lett. A 285 (2001) 191
[3] S. B. Wilkins et al., Phys. Rev. B 73 (2006) 060406R
[4] H. C. Walker et al., Phys. Rev. Lett. 97 (2006) 37203
[5] T. Matsumara et al., Phys. Rev. B 65, (2002) 094420
[6] T. Matsumura et al., Phys. Rev. Lett. 103, (2009) 017203

Experimental Aspects

Experimental aspects

General considerations / X-ray magnetic scattering

- The technique requires the energy tuneability and high flux available at 3rd generation synchrotron sources, as well as full polarization control and polarization analysis
- Horizontal scattering geometry >> vertical scattering geometry $\Rightarrow$ dedicated diffractometers
- The possibility of achieving a very small beam focus allows to investigate very small crystals and to map out domains;
- The high q resolution allows to investigate disorder near phase transitions
- Exotic phenomena occur mostly at low temperatures in magnetic and strongly correlated electron systems; they are very sensitive to external perturbations such as electric field, magnetic field or pressure $\Rightarrow$ many different type of sample environments

Experimental aspects

Dedicated beamlines at 3rd generation synchrotron sources

Resonant scattering and diffraction beamline P09 at PETRA III at DESY

Energy range 3.0 till 14 keV w/ focus and full polarization control;

- EH1: High precision “4S+2D” 6-circle diffractometer

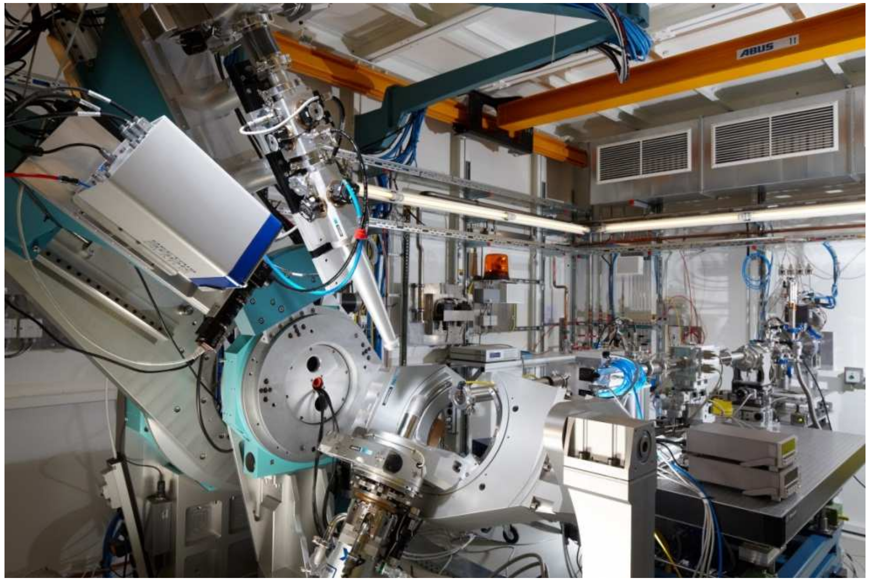

- EH2: non-magnetic heavy-load 6-circle diffractometer in horizontal Psi geometry
  - ✓ 14 Tesla magnet w/ different probes: he-3 & rotator
  - ✓ High pressure

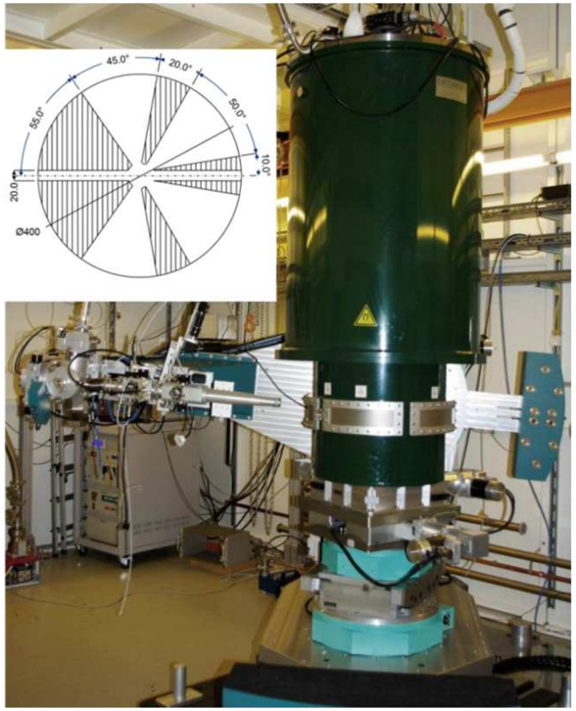

Experimental aspects

Dedicated beamlines at 3rd generation synchrotron sources

Resonant scattering and diffraction beamline P09 at PETRA III at DESY

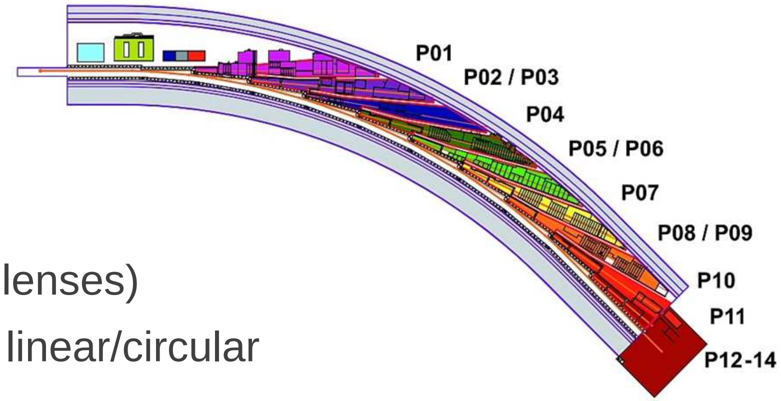

Monochromator: DCM Si-(111)/(311)

Energy range: 2.7 – 24 (50) keV

Flux at 10 keV: 2×10^{13} counts/sec

Focus size (moderate): 140 x 40 μm^2 (mirror)

(small): 40 x 4 μm^2 (compound refractive lenses)

Variable incident polarization: double phase plates, linear/circular

Energy resolution: < 1 eV, <0.3 eV

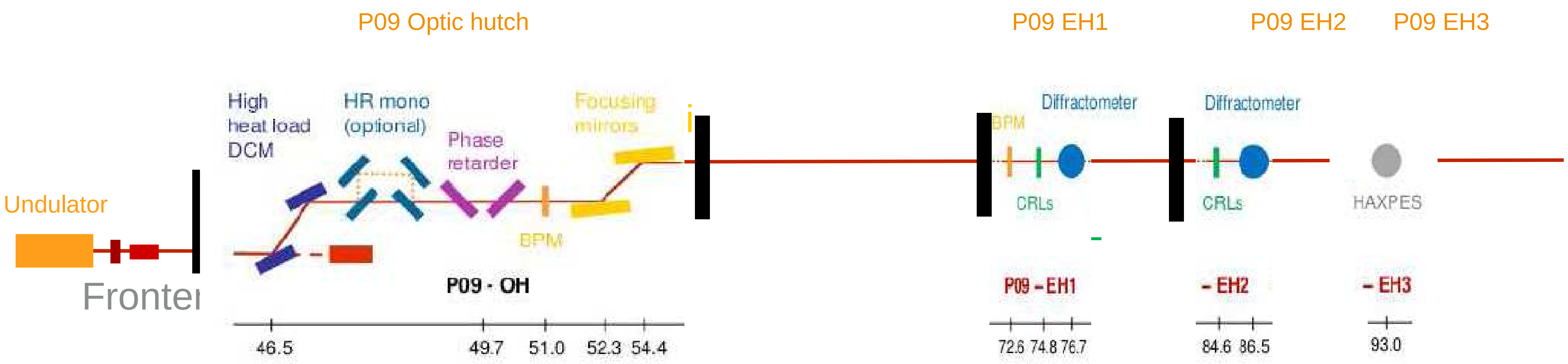

Experimental aspects

Stokes parameters

$P_2 = 1, P_1 = P_3 = 0$ $\quad$ $P_3 = 1, P_1 = P_2 = 0$ $\quad$ $P_1 \neq P_2 \neq P_3 \neq 0$

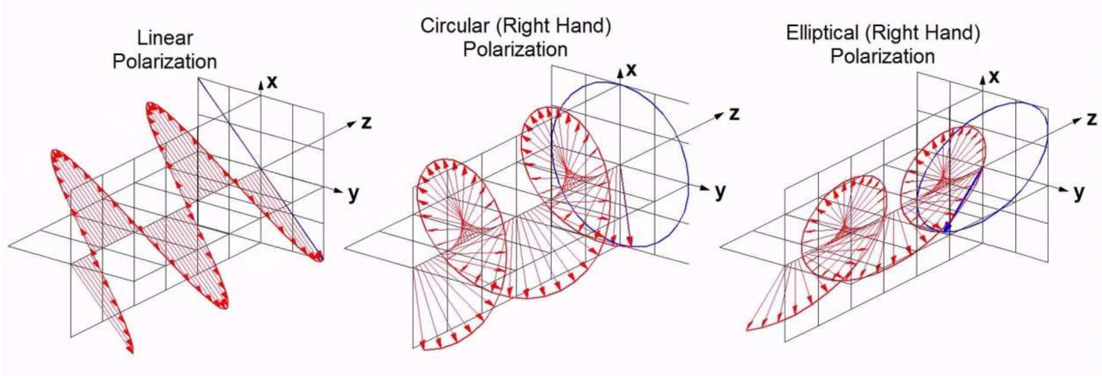

Measurable quantities: Stokes parameters

$$
\begin{aligned}
P_1 &= (|E'_\sigma|^2 - |E'_\pi|^2)/P_0 \\
P_2 &= 2\mathrm{Re}(E'^*_\sigma E'_\pi)/P_0 \\
P_3 &= 2\mathrm{Im}(E'^*_\sigma E'_\pi)/P_0
\end{aligned}
$$

$$P_1^2 + P_2^2 + P_3^2 \leq 1$$

$$P_{LIN} = \sqrt{{P_1}^2 + {P_2}^2}$$

Analyzer crystals scattering at 90 degrees for Polarization analysis

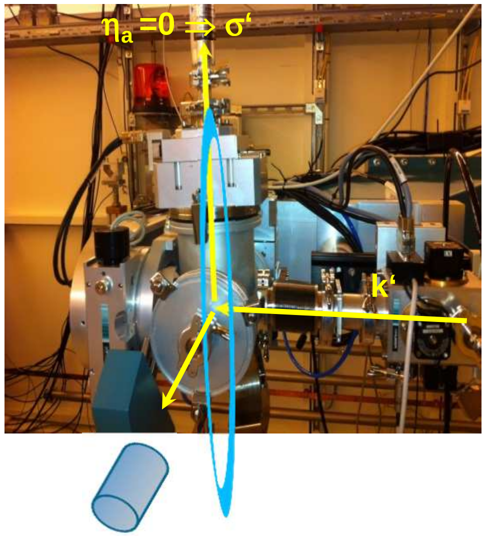

$$I_{\mathrm{int}}(\eta_a) = I_0 * (1 + \cos^2 2\theta_{B,a} + P_{LIN} * \cos 2(\eta_a - \eta) * \sin^2 2\theta_{B,a})$$

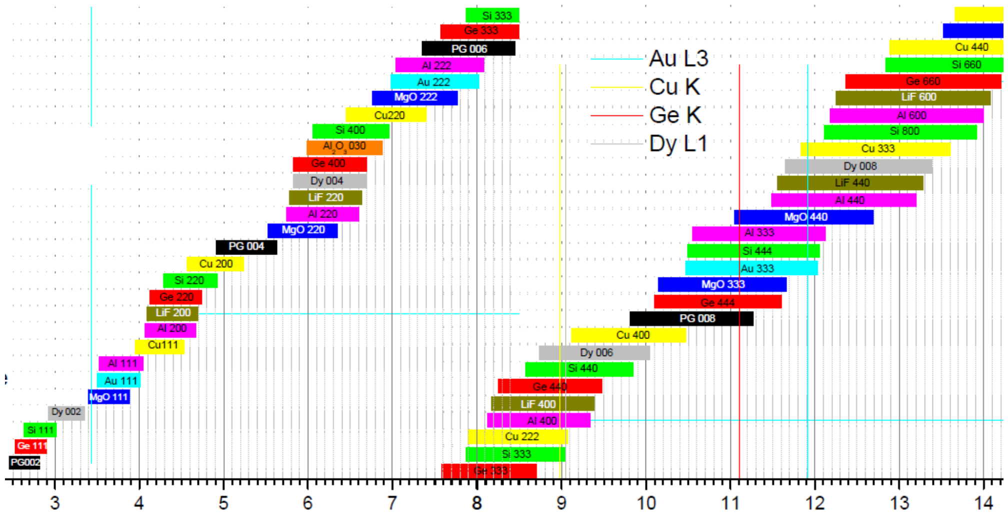

Experimental aspects

Azimuthal scans and polarization analysis

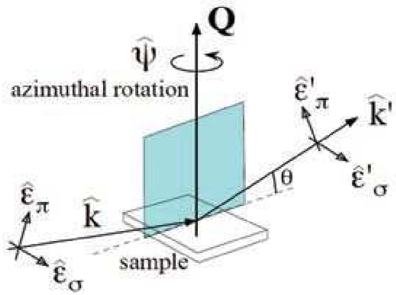

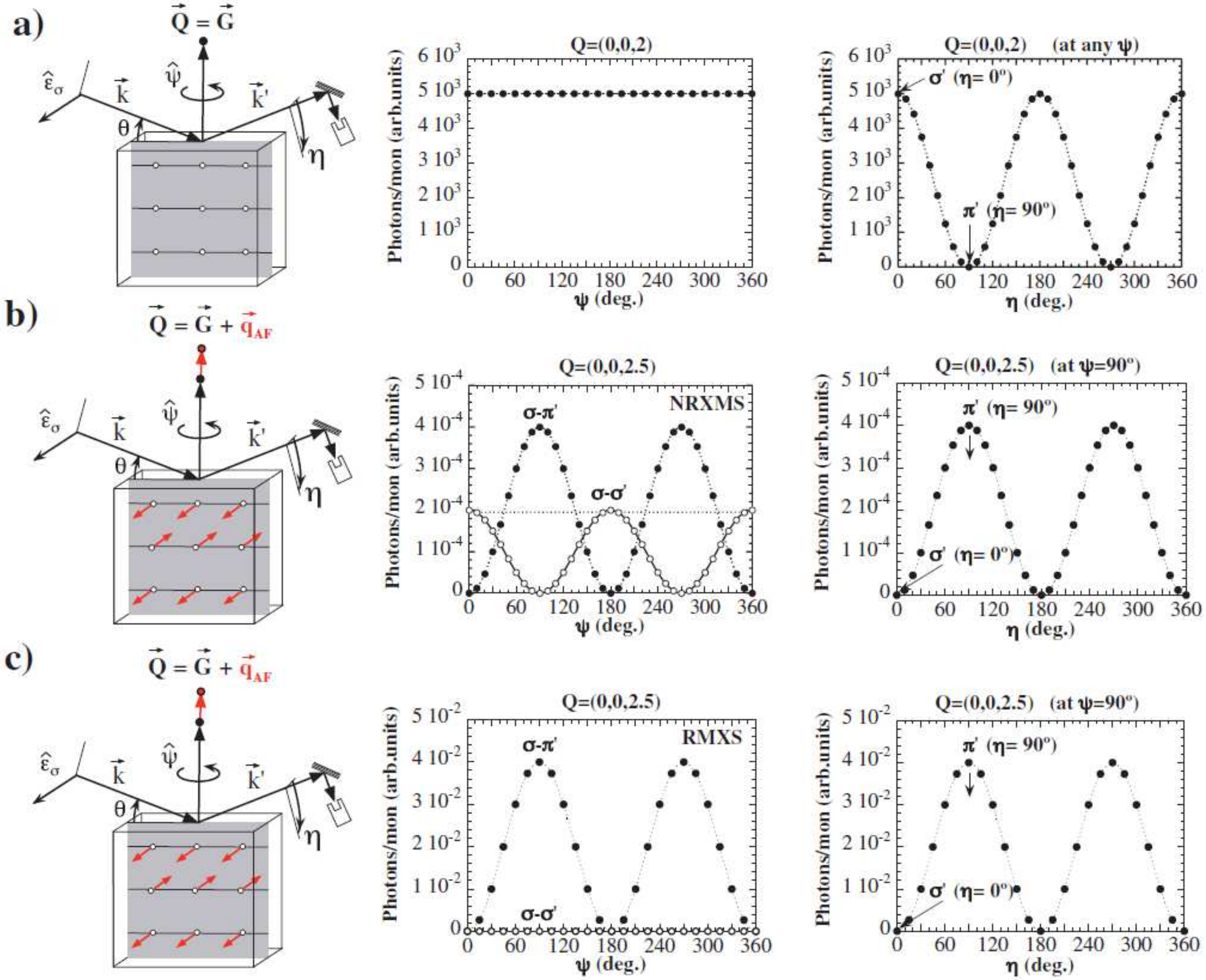

$$F^{(0)}\begin{pmatrix} 1 & 0 \\ 0 & \cos 2\theta \end{pmatrix}$$

$$f^{magn.}_{\sigma-\sigma'} \propto S_2 \sin 2\theta = S \sin 2\theta \cos\psi$$

$$f^{magn.}_{\sigma-\pi'} \propto 2\sin^2\theta\,[\cos\theta\,(L_1 + S_1) + S_3 \sin\theta] = \cos\theta\,(L + S)\sin\psi$$

$$\begin{pmatrix} 0 & z_1\cos\theta + z_3\sin\theta \\ z_3\sin\theta - z_1\cos\theta & -z_2\sin 2\theta \end{pmatrix}$$

Experimental aspects

Dichroic studies

Circular left and right combined with azimuthal scans in resonant X-ray scattering can be used to determine the exact structure of magnetic spin conical spirals

S. L. Zhang *et al.*, Phys. Rev. B 96, 094401 (2017)

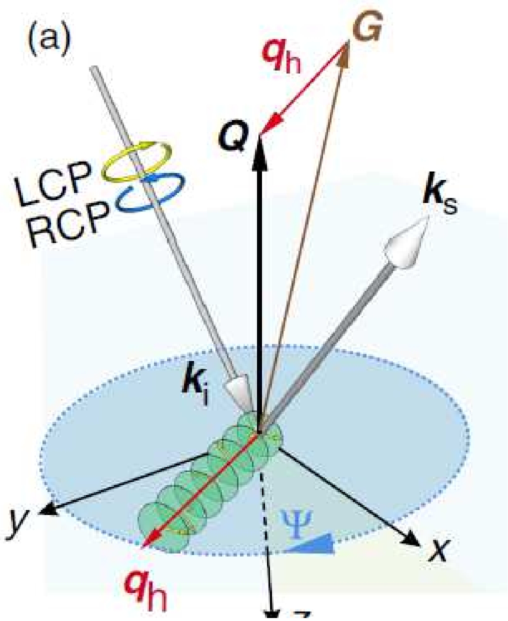

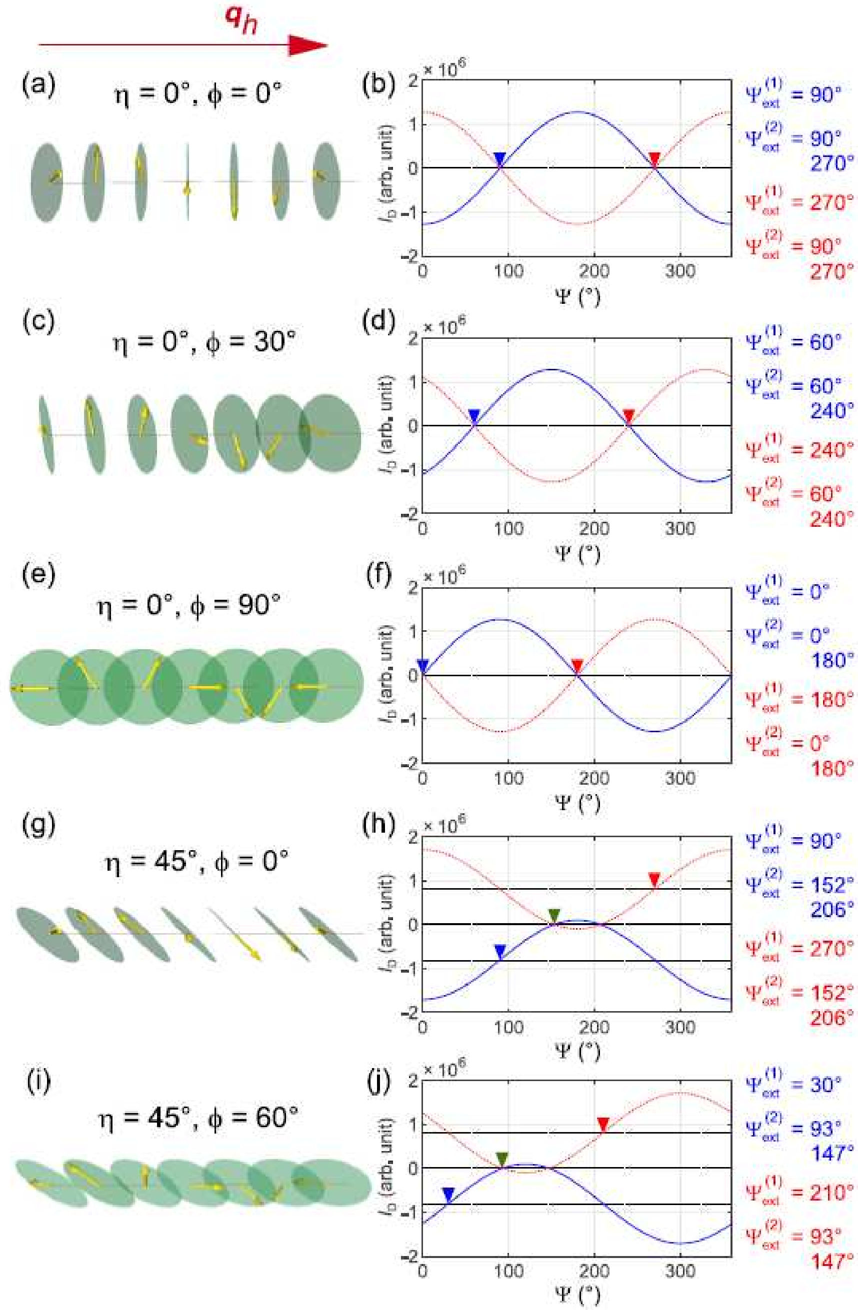

Experimental aspects

Birefringence and Wave plates

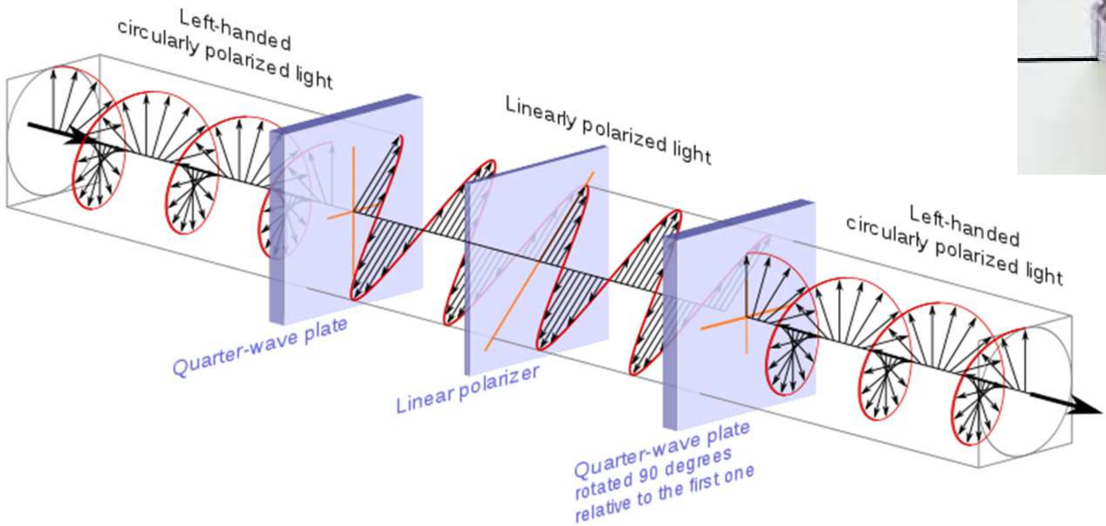

Unpolarized light entering a birefringent crystal not along the optic axis of the crystal is split into 2 beams which are refracted by different amounts.

The components of **E** parallel and perpendicular to optic axis emerge with a phase difference δ between them given by $\delta = (2\pi d/\lambda)\Delta n$.

- A **quarter-wave plate (QWP)** $\delta = \pi/2$ can be used to convert linearly polarized light to circularly polarized light. The incident linearly polarized light must be oriented at 45º to the wave plate's axes.
- A **half-wave plate (HWP)** $\delta = \pi$ can be used to rotate the plane of linearly polarized light. The angle of rotation is 2θ, where θ is the angle between the angle of polarization and the wave plate's fast axis.

Experimental aspects

Birefringence and Wave plates

Birefringence weak in the X ray wavelength region, indice of refraction ~ 1 and isotropic;
Birefringence near Bragg diffraction (dynamical theory of X-rays)

P. Skalicky and C. Malgrange, Acta Cryst. A 28, 501 (1972)
C. Giles & C. Malgrange , work 1994 till 1999 and references therein

For a 45° angle between the diffracting planes and the electric vector, the phase shift between the s- and p- waves writes as:

$$\phi_{\sigma\pi} = -(\pi/2)*[r_e^2 \lambda_X^3 \mathrm{Re}(F_{\mathbf{G}}F_{-\mathbf{G}}^*) \sin(2\theta_B)]*t_{eff} / [\Delta\theta*(\pi V)^2]$$

- Perfect crystals: diamond, LiF, silicium
- Low Z to maximize transmission and minimize “aberrations”
- Lattice spacing determines minimum energy of use: C(111)~3 keV, Si(111)~ 2keV
- Crystal quality

⇒ **Diamond best figure of merit**

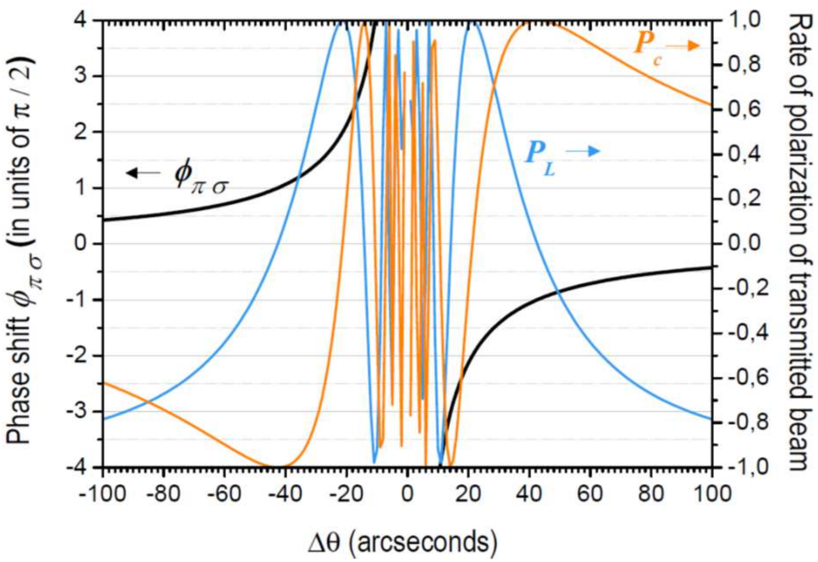

Experimental aspects

Phase retarder plates at beamline P09: 2.7 to 14 keV

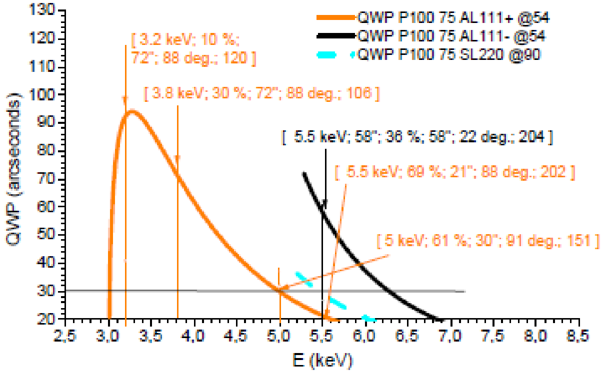

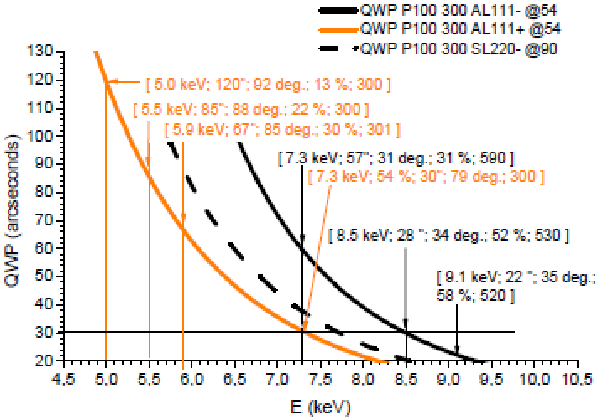

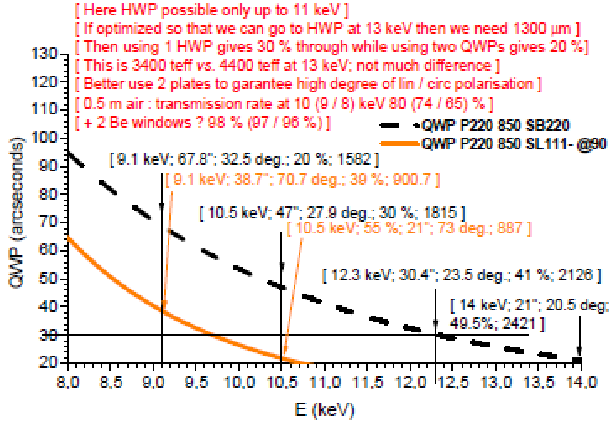

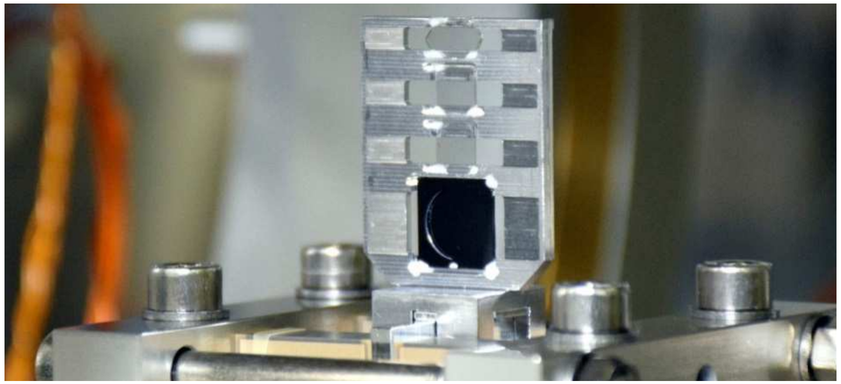

Some recent highlights

Magnetic structure determinations

Full magnetic structure determination $EuPtIn_4$, P09 EH1 4K ARS Cryostat

J. Linares Mardegan *et al.*, *in preparation*

Zintl phases, complex crystallographic structures (extensive polyanionic clusters), semiconductors or semimetals w/ unusual optoelectronic properties and potential for thermoelectric applications;

$EuPtIn_4$@P09, T_N = 13 K;

Magnetic wavevector search: (1/2, 1/2, τ), τ=0.43 incommensurate, 2 atoms per unit cell

Integrated intensities / structure factor calculations $\Rightarrow$ select between Γ_1 and Γ_2 IR

Linear polarization scans $\Rightarrow$ magnetic moment direction $\Rightarrow$ triangulated lattice

Azimuthal scans : unconclusive, travel > 500 µm w/ cryox cryoy

Simulation with mag. moments along (1,-1/2,-1)

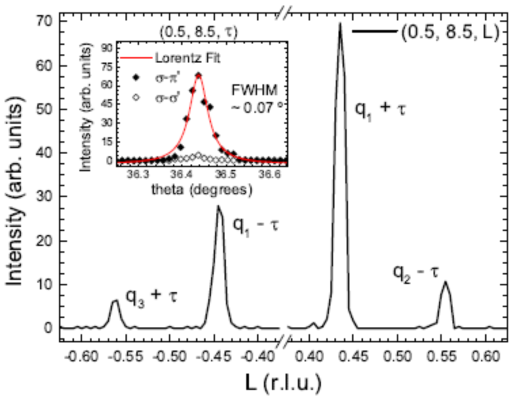

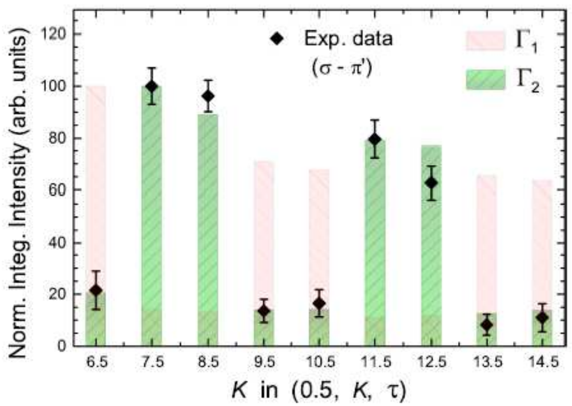

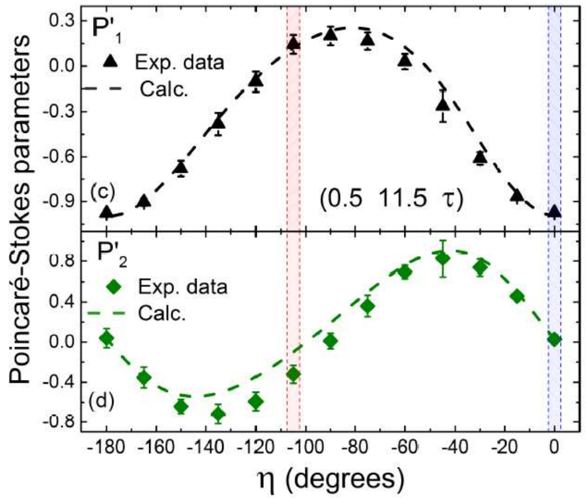

Magnetic structure determinations

Spin Flop transition in $EuPtIn_4$, P09 EH2 14T

J. Linares Mardegan *et al.*, *in preparation*

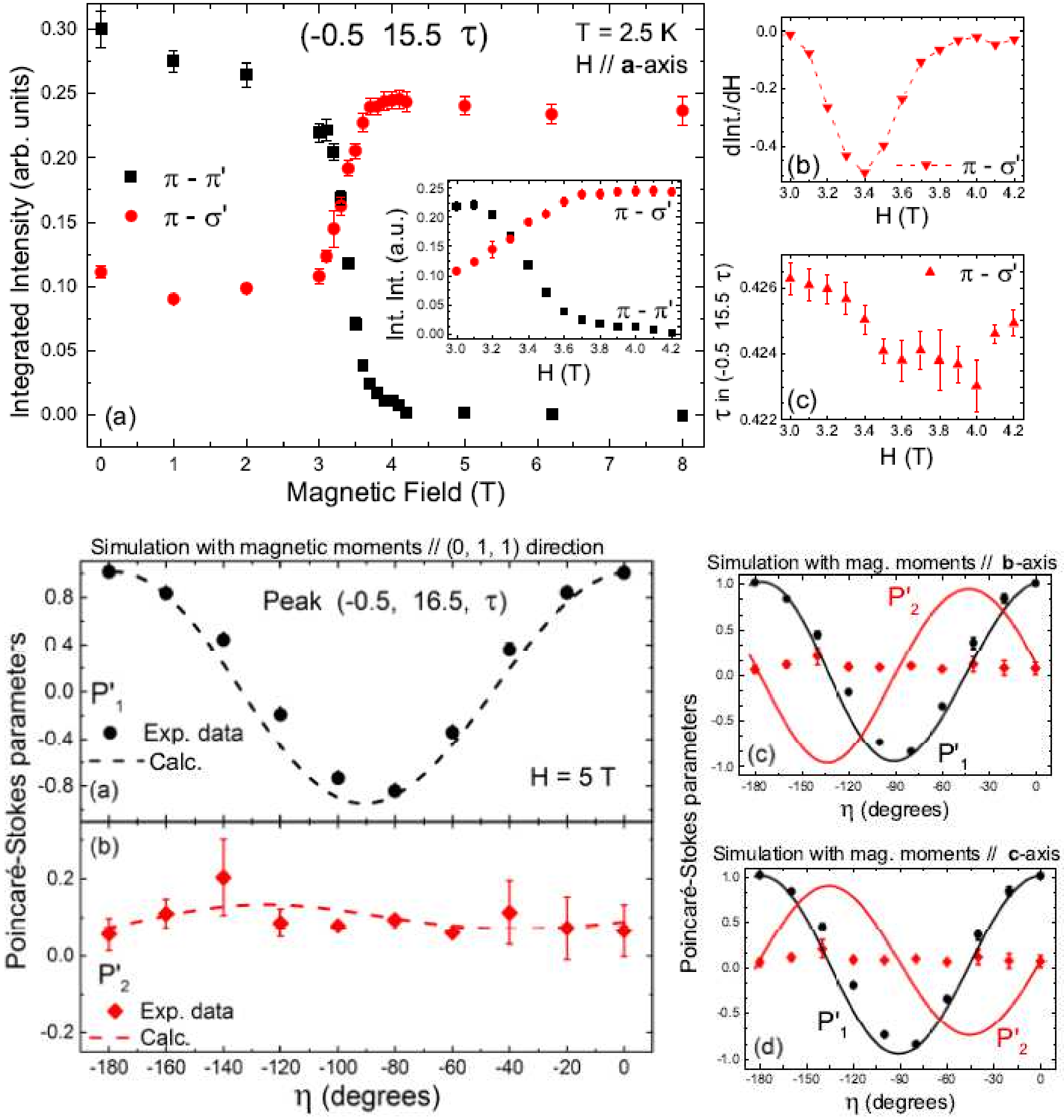

Magnetic structure determinations

All-in all-out magnetic order in $Sm_2Ir_2O_7$, P09 EH1 ARS cryostat

Weyl semimetal exotic state in pyrochlore iridates;

C. Donnerer *et al.*, Phys. Rev. Lett. 117, 037201 (2016)

X. Wan et al., Phys. Rev. B 83, 205101 (2011)

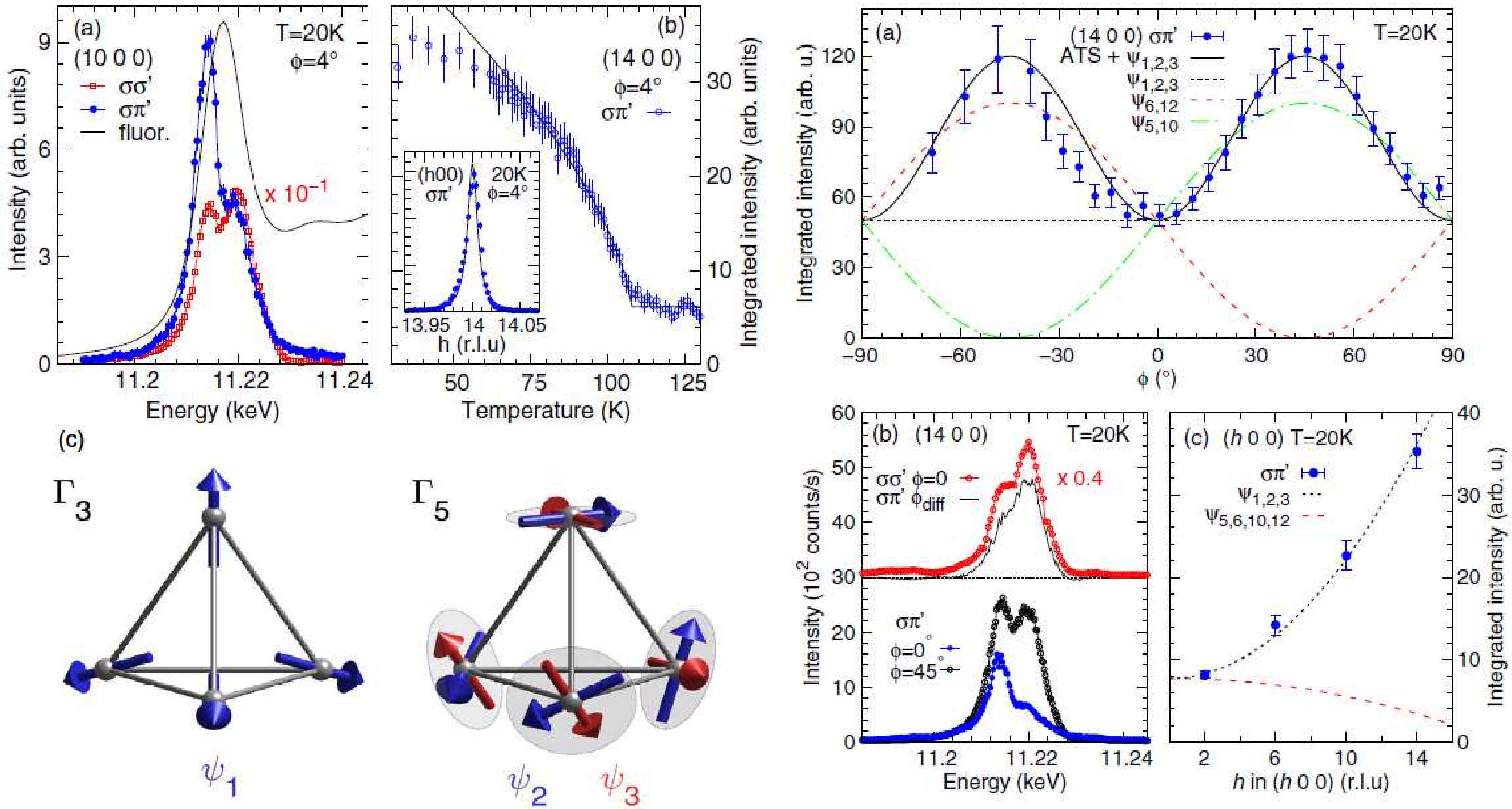

Magnetic structure determination

Ho and Fe magnetic ordering in multiferroic $HoFe_3(BO_3)_4$, P09 EH1 4K ARS Cryostat

D. K. Shukla *et al.*, Phys. Rev. B 86 224421 (2012)

Magnetoelectricity below 23 K, magnetic ordering at 38 K, spin reorientation at 5 K

Azimuthal dependence flat; FPA ⇒ Basal plane spiral in the *(ab)* plane

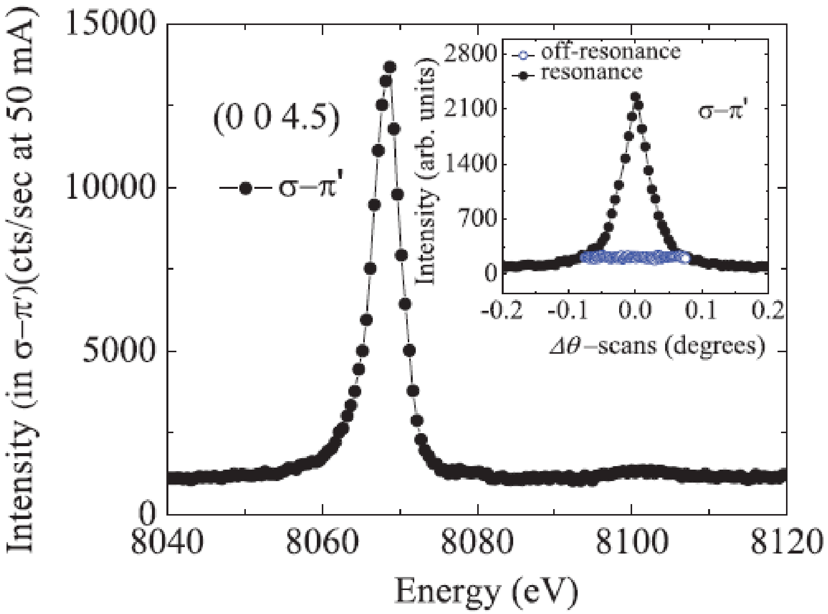

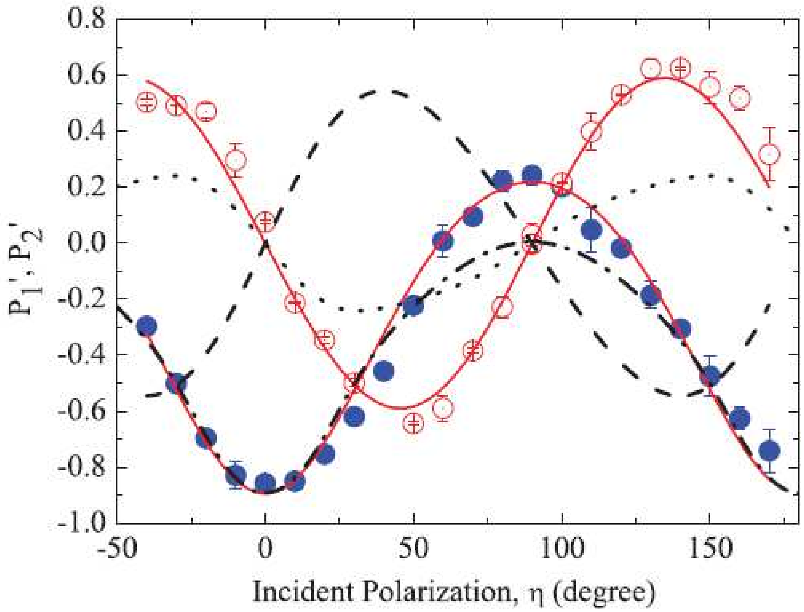

Magnetic structure determination

Ho and Fe magnetic ordering in multiferroic $HoFe_3(BO_3)_4$, P09 & P07

D. K. Shukla *et al.*, Phys. Rev. B 86 224421 (2012)

Magnetoelectricity below 23 K, magnetic ordering at 38 K, spin reorientation at 5 K

Combined high energy magnetic scattering that measures the total spin and RXMS

⇒ Re-arrangement of Fe moments in the basal plane brings magnetoelectricity

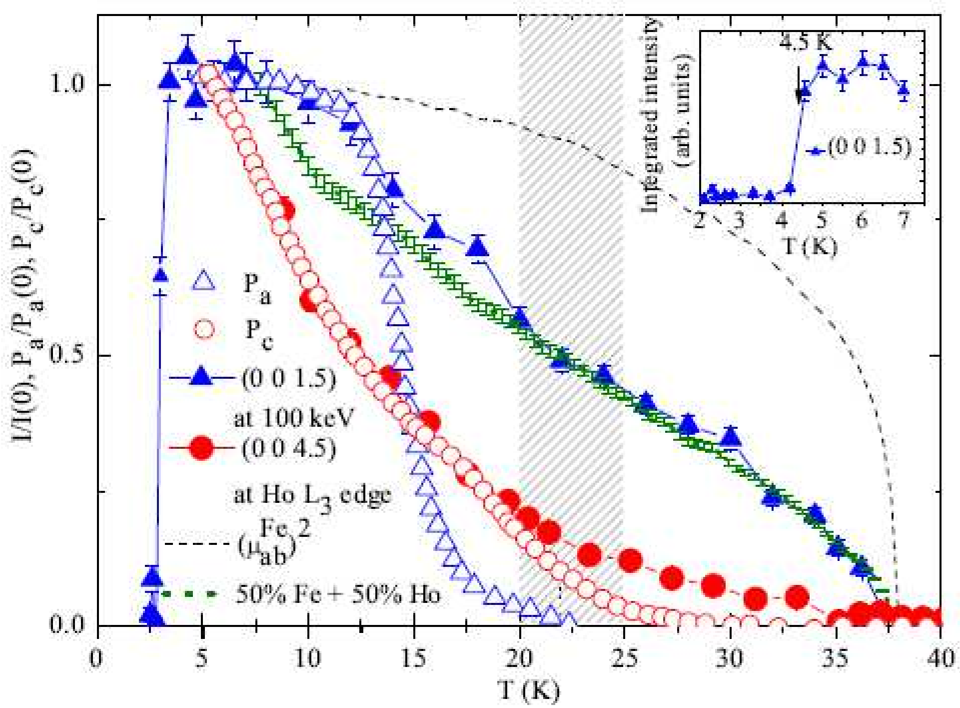

Magnetic X-ray scattering at He-3 temperatures

S. Francoual *et al.*, J. Synchrotron Rad. 22, 1207 (2015)

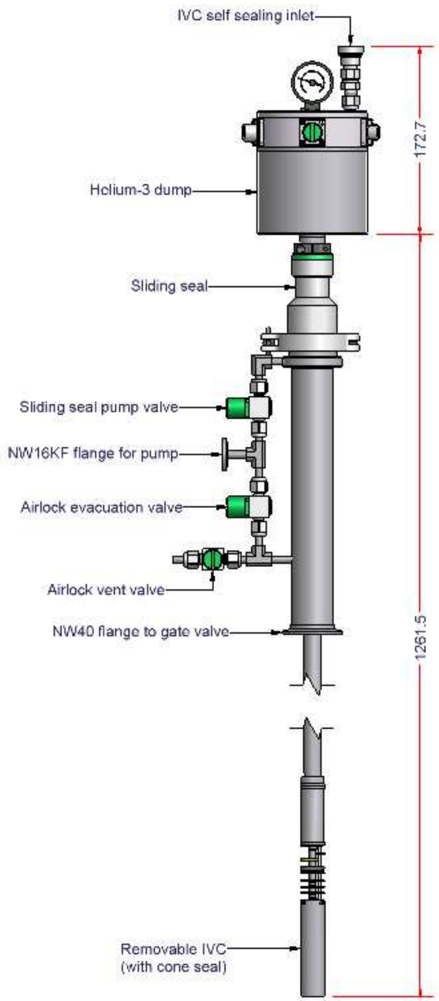

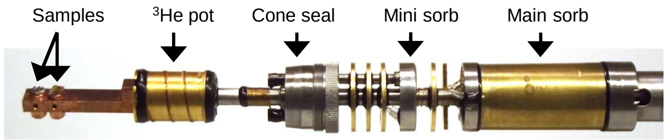

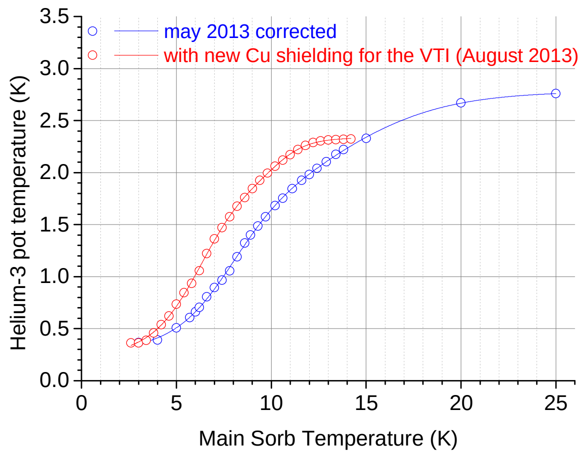

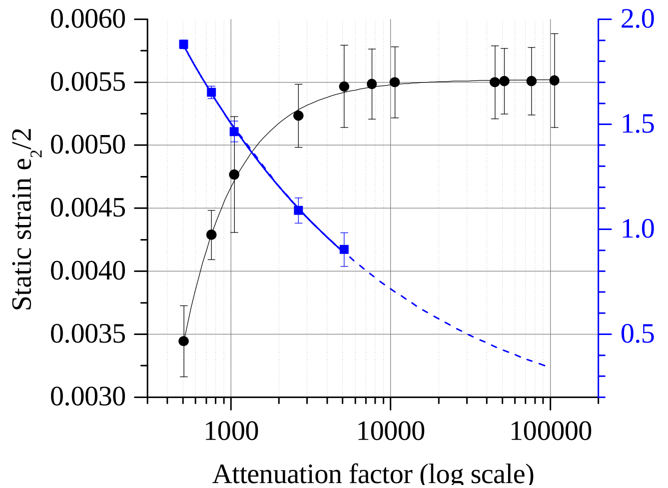

Magnetic X-ray scattering at He-3 temperatures

S. Francoual *et al.*, J. Synchrotron Rad. 22, 1207 (2015)
D. Mannix *et al.*, Physica B 353 121–126 (2004)

$TmNi_2B_2C$, T_{SC}~ 11 K, T_N=1.5 K

Tm moments are aligned along the tetragonal *c*-axis in an incommensurate spin-density wave (SDW)

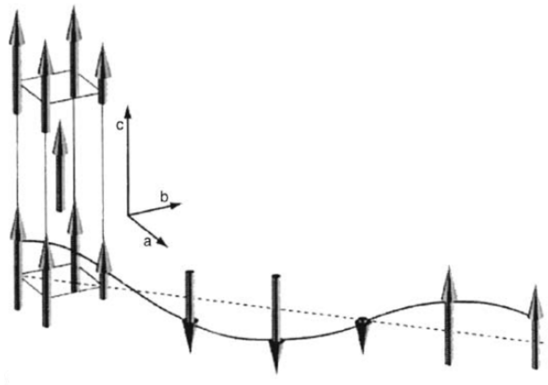

Magnetic satellite observed at the Tm L_3 edge at (1+τ,1+ τ,10), τ=0.0956 in the πσ' channel ⇒ 2.5 counts per second at 360 mK

Analyzer crystal Cu(1,1,1) with 10 % reflectivity, Attenuation factor of 10000 to reduce beam heating effects , Two QWPs in series in a 90º geometry absorbing 50 % + attenuators such that equivalent attenuation factor is 10000, 90 minutes measurement counting 30 seconds / point

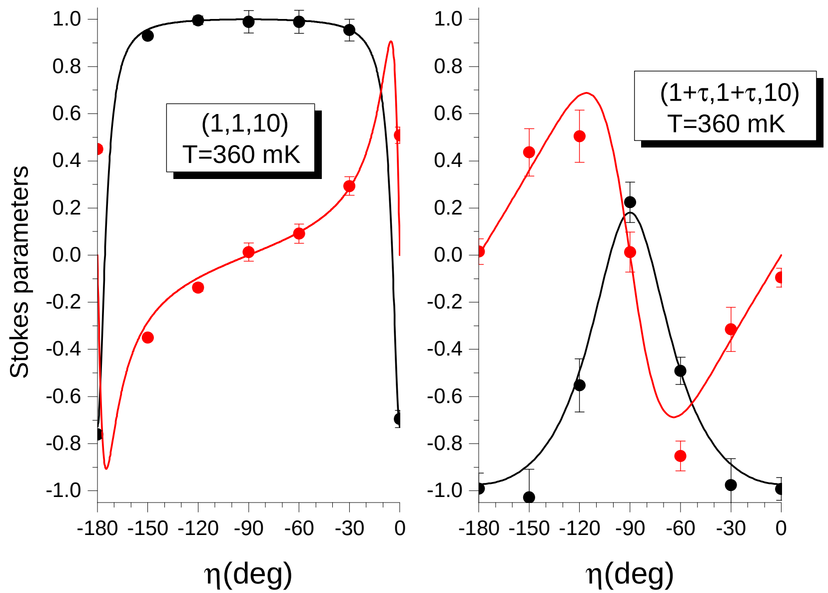

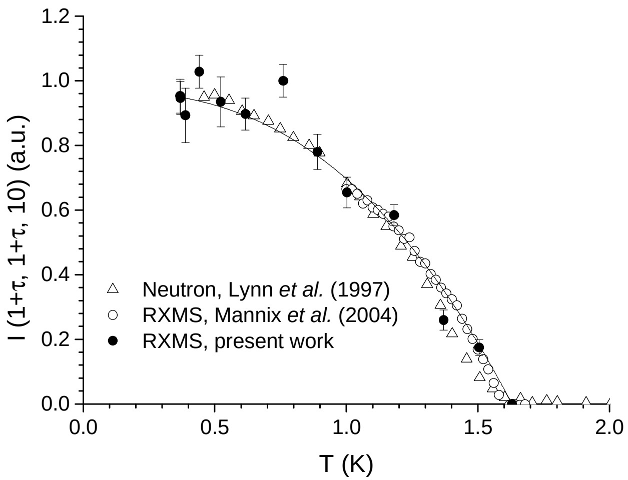

Magnetic X-ray scattering at He-3 temperatures

S. Francoual *et al.*, J. Synchrotron Rad. 22, 1207 (2015)
D. Mannix *et al.*, Physica B 353 121–126 (2004)

$TmNi_2B_2C$, T_{SC}~ 11 K, T_N=1.5 K

Tm moments are aligned along the tetragonal *c*-axis in an incommensurate spin-density wave (SDW)

Magnetic satellite observed at the Tm L_3 edge at (1+τ,1+ τ,10), τ=0.0956 in the πσ' channel ⇒ 2.5 counts per second at 360 mK

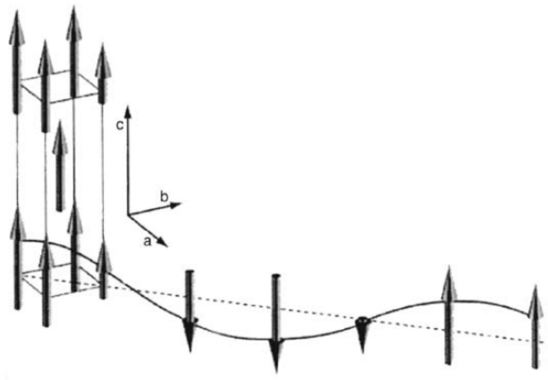

Analyzer crystal Cu(1,1,1) with 10 % reflectivity, Attenuation factor of 10000 to reduce beam heating effects , Two QWPs in series in a 90º geometry absorbing 50 % + attenuators such that equivalent attenuation factor is 10000, 90 minutes measurement counting 30 seconds / point

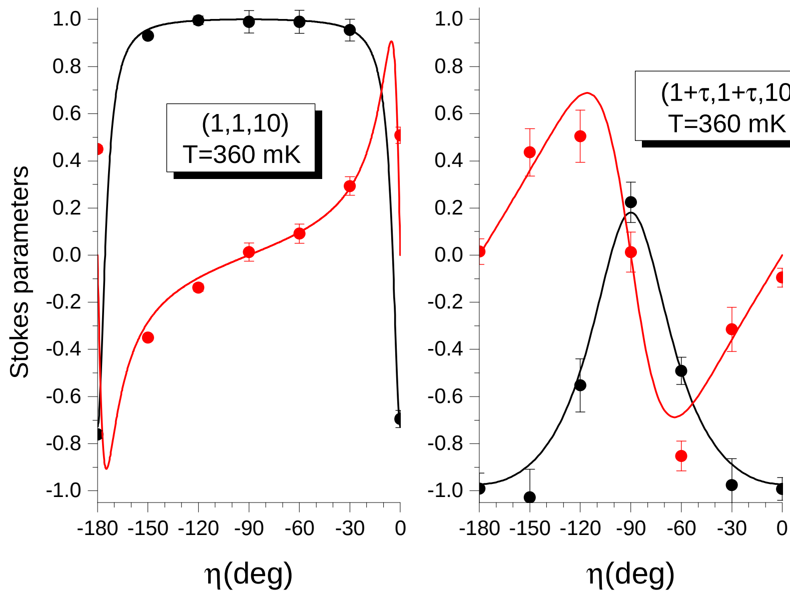

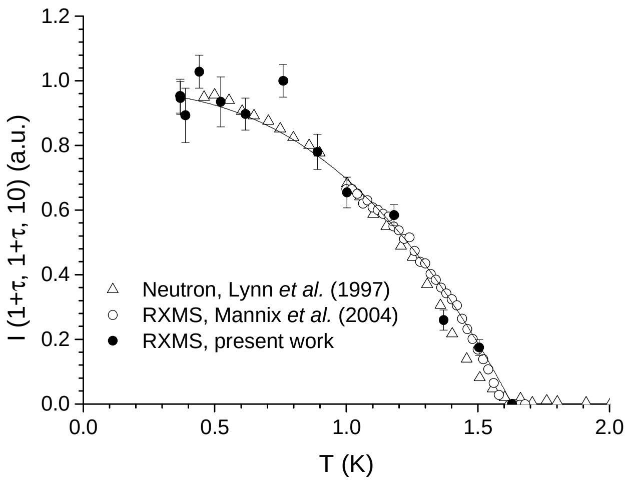

Conclusions

Conclusions

Non-resonant magnetic x-ray scattering:
- Determination of L/S ratio of ordered magnetic phases

Resonant X-ray scattering:
- Chemical and shell selectivity
- High order multipoles, orbital ordering, local site anisotropies

Both full magnetic structure determinations & magnetic domain imaging

X-ray polarization analysis and control w/ or w/o azimuthal dependences
- Single out the individual scattering amplitude contributions
- Complex sample environments
- Dichroic studies

Thank you for your attention !